White matter basis for the hub-and-spoke semantic representation: evidence from semantic dementia

Yan Chen,[1,2,*] Lin Huang,[3,*] Keliang Chen,[4] Junhua Ding,[1] Yumei Zhang,[5] Qing Yang,[4] Yingru Lv,[6] Zaizhu Han[1] and Qihao Guo[3]

*These authors contributed equally to this work.

The hub-and-spoke semantic representation theory posits that semantic knowledge is processed in a neural network, which contains an amodal hub, the sensorimotor modality-specific regions, and the connections between them. The exact neural basis of the hub, regions and connectivity remains unclear. Semantic dementia could be an ideal lesion model to construct the semantic network as this disease presents both amodal and modality-specific semantic processing (e.g. colour) deficits. The goal of the present study was to identify, using an unbiased data-driven approach, the semantic hub and its general and modality-specific semantic white matter connections by investigating the relationship between the lesion degree of the network and the severity of semantic deficits in 33 patients with semantic dementia. Data of diffusion-weighted imaging and behavioural performance in processing knowledge of general semantic and six sensorimotor modalities (i.e. object form, colour, motion, sound, manipulation and function) were collected from each subject. Specifically, to identify the semantic hub, we mapped the white matter nodal degree value (a graph theoretical index) of the 90 regions in the automated anatomical labelling atlas with the general semantic abilities of the patients. Of the regions, only the left fusiform gyrus was identified as the hub because its structural connectivity strength (i.e. nodal degree value) could significantly predict the general semantic processing of the patients. To identify the general and modality-specific semantic connections of the semantic hub, we separately correlated the white matter integrity values of each tract connected with the left fusiform gyrus, with the performance for general semantic processing and each of six semantic modality processing. The results showed that the hub region worked in concert with nine other regions in the semantic memory network for general semantic processing. Moreover, the connection between the hub and the left calcarine was associated with colour-specific semantic processing. The observed effects could not be accounted for by potential confounding variables (e.g. total grey matter volume, regional grey matter volume and performance on non-semantic control tasks). Our findings refine the neuroanatomical structure of the semantic network and underline the critical role of the left fusiform gyrus and its connectivity in the network.

1 State Key Laboratory of Cognitive Neuroscience and Learning and IDG/McGovern Institute for Brain Research, Beijing Normal University, Beijing 100875, China
2 College of Biomedical Engineering and Instrument Sciences, Zhejiang University, Hangzhou 310027, China
3 Department of Gerontology, Shanghai Jiao Tong University Affiliated Sixth People's Hospital, Shanghai 200233, China
4 Department of Neurology, Huashan Hospital, Fudan University, Shanghai 200040, China
5 Department of Radiology, Beijing Tiantan Hospital, Capital Medical University, Beijing 100050, China
6 Department of Radiology, Huashan Hospital, Fudan University, Shanghai 200040, China

Correspondence to: Zaizhu Han
State Key Laboratory of Cognitive Neuroscience and Learning and IDG/McGovern Institute
for Brain Research, Beijing Normal University, Beijing 100875, China
E-mail: zzhhan@bnu.edu.cn

Correspondence may also be addressed to: Qihao Guo
Department of Gerontology, Shanghai Jiao Tong University Affiliated Sixth People's Hospital,
Shanghai 200233, China
E-mail: qhguo@sjtu.edu.cn

Introduction

Semantic memory refers to the general knowledge of objects, people, facts and word meanings (Tulving, 1972; Warrington and Shallice, 1984; Rogers *et al.*, 2004; Martin, 2016), which partly supports a wide range of other cognitive processes (e.g. language comprehension and object recognition). The representation of semantic memory in the human brain has been widely explored (Patterson *et al.*, 2007; Binder *et al.*, 2009; Lambon Ralph *et al.*, 2016). To date, empirical findings tend to support the hub-and-spoke theory of semantic representation (Patterson *et al.*, 2007; Schapiro *et al.*, 2013; Rice *et al.*, 2015a). This theory posits that a semantic concept (e.g. cat) consists of knowledge of various sensorimotor attributes (e.g. form, colour, motion, sound, function). The knowledge is stored in the brain regions responsible for processing these modality attributes (i.e. modality-specific regions; Martin, 2007). Moreover, information from different modalities is further bound together to form an amodal semantic concept in a semantic hub (Lambon Ralph *et al.*, 2010). Thus, one would expect that damage to the semantic hub region leads to general semantic processing deficits regardless of modalities, whereas damage to the modality-specific cortical regions would cause deficits in the corresponding modality processing (Patterson *et al.*, 2007).

Recent studies on brain-damaged patients, especially those with semantic dementia, have provided converging evidence for the hub-and-spoke semantic representation theory (Patterson *et al.*, 2007; Mion *et al.*, 2010; Guo *et al.*, 2013; Lambon Ralph *et al.*, 2016). Semantic dementia is an ideal lesion model to reveal the organizational principle of the semantic system. This disease is characterized by a core symptom of selective and degenerative semantic impairments with relative sparing of other cognitive abilities (e.g. speech production, episodic memory and executive function) (Warrington and Shallice, 1984; Snowden *et al.*, 2004; Mesulam *et al.*, 2012) due to their relatively focal brain grey matter atrophy and white matter pathology (Acosta-Cabronero *et al.*, 2011; Andreotti *et al.*, 2017). Patients with semantic dementia show general semantic deficits in every sensorimotor and verbal modality, including words (Jefferies *et al.*, 2009), sounds (Golden *et al.*, 2015), smells (Luzzi *et al.*, 2007) and motor knowledge (Lin *et al.*, 2011). This indicates that patients with semantic dementia exhibit amodal semantic disruption, thus providing evidence for the existence of a semantic hub. Other studies have further observed that patients with semantic dementia also display a disproportional loss of knowledge for some given modalities. Hoffman *et al.* (2012), for example, observed that the patients had an advantage for naming objects with rich sound/motion and tactile/action information but not for objects with rich colour/shape information. Indeed, the richness of colour/shape knowledge even had an increasingly negative impact in the later stages of the disorder. These findings demonstrate that, in addition to amodal semantic disruption, patients with semantic dementia also exhibit modality-specific semantic (e.g. colour/shape) impairments.

Given that the semantic system is organized as a neural network in which a hub is connected with sensorimotor modality regions, two relevant questions for this theory are raised: where the hub region is and how the hub connects with the modality-specific semantic regions. Regarding the first question, although converging evidence has shown that the hub region lies within the anterior temporal lobe (ATL) (Patterson *et al.*, 2007; Lambon Ralph, 2014; Rice *et al.*, 2015b, 2018), it remains controversial which area is the hub region because the ATL includes several areas [e.g. temporal pole, fusiform gyrus (FFG), superior temporal gyrus, middle temporal gyrus and inferior temporal gyrus]. Some studies have supported that the hub is localized in the temporal pole, which is the most severe atrophic region in semantic dementia individuals. The relevant evidence has been mainly derived from the fact that the atrophic degree of the temporal pole in semantic dementia or temporary dysfunction of this region in healthy subjects was significantly associated with multimodal semantic deficits (Pobric *et al.*, 2007; Butler *et al.*, 2009; Lambon Ralph *et al.*, 2009). However, others have positioned the hub in other regions of the ATL (Binney *et al.*, 2010; Mion *et al.*, 2010; Rice *et al.*, 2015b; Ding *et al.*, 2016). For instance, Mion *et al.* (2010) conducted a whole-brain regression analysis, and revealed that the semantic impairments of patients with semantic dementia were best predicted by hypometabolism in the FFG. To our knowledge, previous studies have identified the hub region mainly by investigating the effects of individual regions in isolation, without considering the contribution of modality-specific regions to the hub. As the semantic hub works in the form of a network, it is optimal to identify the hub from a network connectivity perspective (Freeman, 1977; Achard *et al.*, 2006). Regarding the second question, the literature has revealed some semantic-associated white matter bundles

in patients with semantic dementia (e.g. the inferior longitudinal fasciculus and the arcuate fasciculus) (Agosta et al., 2010). However, it is unclear whether these tracts are linked between the semantic hub and modality-specific regions.

The present study adopted a data-driven approach to identify the semantic hub and its white matter connectivity with modality-specific regions in the brain network based on 33 patients with semantic dementia. First, to identify the hub region, we correlated the general semantic performance with the nodal degree of the regions in the whole-brain white matter network in the patients. Then, to explore the connectivity from the hub to modality-specific regions, we correlated the general and modality-specific semantic performance with the integrity metrics of each white matter tract connected with the hub region. Finally, the results were further verified by statistically removing the effects of potential confounding variables (e.g. total grey matter volume, grey matter volume of regions of interest, and performance on non-semantic control tasks).

Materials and methods

Participants

Patients with semantic dementia and healthy control subjects took part in the current study. The cohort was identical to that of our recent study (Chen et al., 2019). All participants were right-handed, native Chinese speakers and provided written informed consent. This study was approved by the Institutional Review Board of the Huashan Hospital affiliated with Fudan University.

Patients with semantic dementia

Thirty-three patients with semantic dementia (15 males; age: 62.27 ± 7.49 years; educational level: 11.73 ± 3.01 years) were recruited from the neurology department of Huashan Hospital in Shanghai, China from 2011 to 2018. They had normal or corrected-to-normal hearing and vision, and no history of alcoholism, head trauma, psychiatric or other neurological illness. The neuropsychological performance and predominant ATL atrophy of each patient met the diagnostic criteria for semantic dementia (Gorno-Tempini et al., 2011; see details in the Supplementary material). Sixteen of the patients showed left-lateralized atrophy and 17 showed right-lateralized atrophy (Supplementary Table 1). The Chinese version of the Mini-Mental State Examination (MMSE; Folstein et al., 1975) was used to evaluate the general cognitive state of the patients (21.91 ± 4.01).

Healthy control subjects

Twenty healthy control subjects (eight males; age: 60.50 ± 3.95 years; educational level: 10.45 ± 2.89 years) were recruited from the local community through advertisements. They also had normal or corrected-to-normal hearing and vision, and no history of alcoholism, head trauma, psychiatric or neurological illness. The MMSE scores were 28.10 ± 1.37.

The patients and healthy controls were comparable in age, gender distribution and educational years (P-values > 0.05), while the patients had lower MMSE scores than healthy controls ($t = -8.12$, $P < 0.001$).

Behavioural data collection

We designed six general semantic tasks and six modality-specific semantic tasks (Table 1). The former tasks (oral picture naming, oral sound naming, picture associative matching, word associative matching, word-picture verification, and naming to definition) examined the general aspect of semantic knowledge with various modalities of input and output. The latter tasks assessed subjects' semantic knowledge on six sensorimotor modalities of objects (i.e. form, colour, motion, sound, manipulation and function). Each modality task consisted of a verbal subtask and a non-verbal subtask. We also included three non-semantic control tasks (visual perception, sound perception and number proximity matching), which involved no or minimal semantic processing. The procedures of these tasks are explained in detail in the Supplementary material.

Behavioural data preprocessing

Because patients showed considerable variation in demographic properties (e.g. age, gender and education), their raw scores from the behavioural tasks might not meaningfully reflect the degree of deficit. To obtain an index that could more precisely measure the deficits, we used the single case-to-controls method proposed by Crawford and Garthwaite (2006): the patients' raw behavioural scores were corrected by considering the performance and demographic information of the 20 healthy subjects and transformed into standardized t-scores (for a detailed description of this method, see Han et al., 2013).

To determine the general semantic ability of the patients, a principal component analysis (PCA) was conducted based on the six general semantic tasks and three control tasks. Specifically, the patients' t-scores on these nine tasks were entered into a PCA of SPSS 20.0. The semantic PCA factor was defined as a component that had a high loading weight on the tasks in which semantic processing was highly relevant, i.e. the six general semantic tasks. The scores corresponding to this factor were considered to reflect the general semantic processing of the patients with semantic dementia.

Imaging data collection

All participants were scanned on a 3 T Siemens scanner at Huashan Hospital. 3D T_1-weighted images and diffusion-weighted images were collected. T_1 images were obtained with a magnetization prepared rapid gradient echo (MPRAGE) sequence along the sagittal plane with the parameters: repetition time = 2300 ms, echo time = 2.98 ms, flip angle = 9°, matrix size = 240 × 256, field of view = 240 × 256 mm², slice number = 192 slices, slice thickness = 1 mm, voxel size = 1 × 1 × 1 mm³. The sequence for

Table 1 Behavioural performance of the participants

Tasks	Raw accuracy: mean (SD)		Corrected t-scores (SD) of patients
	Healthy controls	**Semantic dementia**	
General semantic task			
Oral picture naming	90% (5%)	32% (19%)	−9.69 (3.31)
Oral sound naming	75% (12%)	23% (14%)	−3.85 (1.33)
Picture associative matching	95% (3%)	73% (10%)	−5.32 (2.36)
Word associative matching	96% (2%)	75% (12%)	−15.15 (9.11)
Word-picture verification	96% (3%)	61% (22%)	−11.39 (7.52)
Naming to definition	83% (8%)	24% (18%)	−9.52 (2.94)
Modality-specific semantic task			
Verbal task			
Form matching	93% (4%)	74% (13%)	−4.53 (3.05)
Colour matching	95% (4%)	68% (13%)	−5.09 (2.39)
Motion matching	92% (5%)	66% (13%)	−3.76 (2.62)
Sound matching	82% (8%)	67% (8%)	−1.56 (0.76)
Manipulation matching	92% (5%)	69% (16%)	−5.68 (2.69)
Function matching	98% (2%)	79% (12%)	−11.31 (7.13)
Non-verbal task			
Form verification	81% (7%)	51% (15%)	−4.20 (2.05)
Colour verification	71% (10%)	38% (15%)	−2.76 (1.30)
Motion verification	57% (13%)	34% (16%)	−0.46 (1.41)
Sound verification	78% (9%)	35% (15%)	−3.87 (1.38)
Manipulation matching	76% (9%)	72% (16%)	−1.66 (1.24)
Function matching	91% (6%)	76% (10%)	−2.16 (1.47)
Non-semantic control task			
Visual perception	91% (5%)	92% (6%)	−0.96 (1.02)
Sound perception	88% (10%)	76% (13%)	0.13 (0.86)
Number proximity matching	93% (14%)	92% (6%)	−0.23 (1.43)

diffusion-weighted images was scanned twice in the transverse plane with the parameters: 20 diffusion weighting directions with $b = 1000$ s/mm^2, one additional image without diffusion weighting (i.e. $b = 0$ image), repetition time = 8500 ms, echo time = 87 ms, flip angle = 90°, matrix size = 128×128, field of view = 230×230 mm^2, slice number = 46 slices, slice thickness = 3 mm, voxel size = $1.8 \times 1.8 \times 3$ mm^3.

Imaging data preprocessing

T$_1$ imaging data

T$_1$ images were first segmented into grey matter, white matter and CSF with a $1.5 \times 1.5 \times 1.5$ mm^3 resolution using the voxel-based morphometry (VBM8) toolbox in SPM8 (https://www.fil.ion.ucl.ac.uk/spm/software/spm8/). The output images were then normalized into Montreal Neurological Institute (MNI) space using the Diffeomorphic Anatomical Registration Through Exponentiated Lie algebra (DARTEL) registration method (Ashburner, 2007). The grey matter images were further modulated and smoothed with an 8-mm full-width at half-maximum Gaussian kernel to obtain the grey matter volume images. To illustrate the brain atrophy of the patients, an independent-sample t-test was performed to compare the grey matter volume of each voxel in the whole brain between semantic dementia patients and healthy controls with a threshold of false discovery rate (FDR) corrected $q < 0.01$.

Diffusion-weighted imaging data

The diffusion-weighted imaging data of each participant were preprocessed using a pipeline tool for analysing brain diffusion images (PANDA; Cui *et al.*, 2013) with the following steps: (i) Estimating the brain mask. Brain mask was estimated by removing the skull from the $b = 0$ image. To achieve this, PANDA used the *bet* command of FMRIB Software Library (FSL); (ii) Correcting for the eddy-current effect. Eddy-current induced distortion of diffusion-weighted images, as well as simple head motion, was corrected by registering the diffusion-weighted images to the $b = 0$ image with an affine transformation using the *eddy_correct* command of FSL. The gradient direction of each diffusion-weighted image was then reoriented according to the resultant affine transformations; (iii) Calculating diffusion tensor metrics. The diffusion tensor models were built and individual fractional anisotropy, mean diffusivity, axial diffusivity and radial diffusivity maps were obtained. To do this, the *dtifit* command of FSL was applied; and (iv) Normalizing. Finally, individual images were registered to the MNI space for comparisons across subjects. Here, PANDA first registered individual fractional anisotropy images of the native space to a standard fractional anisotropy template (FMRIB58_FA 1 mm in FSL) and then applied the resultant

warping transformation to write the images of all diffusion metrics (i.e. fractional anisotropy, and mean, axial and radial diffusivity) into the MNI space ($2 \times 2 \times 2$ mm^3). The *fnirt* and the *applywarp* commands of FSL were used.

Brain network construction

We adopted a previous approach (Gong *et al.*, 2009) to reconstruct the whole-brain white matter network in healthy subjects, and then extracted the integrity value of each tract in patients.

Defining grey matter nodes in healthy control subjects

We applied the automated anatomical labelling (AAL) atlas (Tzourio-Mazoyer *et al.*, 2002) to define the grey matter nodes in the white matter network. Specifically, we first parcelled out the entire cerebral cortex into 90 cortical and subcortical regions, each representing a node of the network. Then, each region was dilated (thickened) by three voxels (voxel size = $2 \times 2 \times 2$ mm^3) using the 'fslmaths' tool in FSL. The dilation of two regions stopped once their borders touched so that different regions did not have overlapping voxels. For each healthy subject, the 90 dilated nodes in the MNI space were transformed to the native diffusion space using PANDA. To do this, the T_1 image of each individual was first coregistered to the fractional anisotropy image in the diffusion tensor imaging (DTI) space using a linear transformation. Then, the transformed T_1 image was normalized to the ICBM152 template in the MNI space using a non-linear transformation. Finally, the AAL mask from the MNI space was warped to the DTI native space using the resulting inverse transformation. Note that the T_1 image was used because it provided more precise information about the cerebral gyri and sulci. This information was critical for registering the borders of grey matter subregions.

Tracing white matter tracts in healthy control subjects

Deterministic tractography was performed in the native diffusion space for each healthy subject using the fibre assignment by continuous tracking (FACT) algorithm (Mori *et al.*, 1999). Specifically, fibre tracking was terminated when the angle between two consecutive orientations was $>45°$ or when the fractional anisotropy value was <0.20. Given that the outcome of tractography is affected by the initial position of the seed points within the voxel (Cheng *et al.*, 2012), 100 seeds were randomly selected within each voxel to avoid biases from initial seed positioning. The tracts for every two AAL regions were filtered out if one end point terminated within one region, and the other end point terminated within the other region. In this case, 4005 regional pairs were tested. For each node pair, the filtered-out tract was binarized and then transformed to MNI space. The binary maps of all the healthy subjects in the MNI space were then overlaid to generate a count map. The value of each voxel represented the number of subjects who had fibres on

it. Finally, to determine whether a node pair was anatomically connected, we used a group-level threshold of voxel value $>25\%$ of subjects (i.e. five subjects) and cluster size >300 voxels (2400 mm^3). This threshold has been adopted by other studies (e.g. Fang *et al.*, 2015). The analysis was performed for all node pairs (4005 potential tracts), and only 457 tracts passed the threshold. The sparsity of the resultant network (11.41%) was similar to that reported in the literature (Achard and Bullmore, 2007; Gong *et al.*, 2009; He *et al.*, 2009). Note that the sparsity was a common graph-theoretical index used to describe the density of edges in a network (Achard and Bullmore, 2007).

Extracting the integrity values of the tracts in patients

We masked each tract obtained in the above analysis and extracted the mean fractional anisotropy, and mean, axial and radial diffusivity values of voxels within the tract for each patient with semantic dementia.

Identifying the semantic hub in patients

In the white matter network, we first computed the nodal degree value of each of the 90 regions for each diffusion metric (fractional anisotropy, and mean, axial and radial diffusivity) of each patient. The degree value was obtained by summing the diffusion metric values of all white matter tracts connecting with the node in the whole-brain network. Then, we correlated the general semantic scores (i.e. the semantic PCA scores) with the nodal degree values of each region across 33 patients with semantic dementia (Bonferroni corrected $P < 0.005$). Three demographic variables (age, gender and education level) were included as covariates. The region showing significant correlational effects for at least one DTI measure was considered the semantic hub region.

To examine whether the observed effects of the semantic hub might be driven by other confounding factors, we again correlated the semantic PCA scores with the nodal degree of the hub region across the patients while controlling for the effects of other potential variables: (i) total grey matter volume (measured by the total grey matter volume of all grey matter voxels in the whole brain); (ii) grey matter volume of the hub region (measured by the grey matter volume of grey matter voxels in the semantic hub); and (iii) performance on the non-semantic control tasks (the corrected *t*-scores of the visual perception, sound perception and number proximity matching tasks).

Note that a region with more white matter connections would have a higher DTI metric-based degree value. However, the number of connections for a given region was identical across patients; therefore, the connection number was not treated as an additional covariate in the nodal degree-behaviour correlational analyses.

Identifying the semantic processing-relevant tracts of the semantic hub

To explore how the semantic hub region works in concert with other regions for semantic processing, we investigated the general and modality-specific semantic tracts connecting to the semantic hub.

Identifying the general semantic tracts of the semantic hub

Although the nodal degree value of the semantic hub significantly correlated with general semantic performance of the patients, it might not mean that each of the tracts connecting from the hub was associated with general semantic processing, because the nodal degree value of the hub reflected an overall summation effects of all, but not the individual, connected tracts. In this case, it remains unknown which connected tracts participated in general semantic processing. To address this issue, we computed the correlation between the integrity of each tract of the hub region and the semantic PCA scores across the 33 patients with semantic dementia (Bonferroni corrected $P < 0.05$, significant for at least one metric). Age, gender and educational level were factored out in the analyses.

To determine whether the effects of the observed general semantic tracts were driven by other potential confounding factors, partial correlation analyses were conducted again with the additional covariates: (i) total grey matter volume; (ii) grey matter volume of the hub region; (iii) grey matter volume of the other node; and (iv) t-scores of the three non-semantic control tasks.

Identifying the modality-specific semantic tracts of the semantic hub

To identify the modality-specific semantic structural pathways of the semantic hub, we tested the correlation between the integrity of each tract of the hub region and t-scores of the 12 modality-specific semantic tasks in the patients ($P < 0.005$, significant for at least one metric). To eliminate the influence of demographic factors and general semantic deterioration, three demographic variables and the semantic PCA scores were introduced as covariates in all the analyses.

To validate the effects of the observed connections, the following potential confounding variables were controlled: (i) total grey matter volume; (ii) grey matter volume of the hub region; (iii) grey matter volume of the other node; and (iv) t-scores of the three non-semantic control tasks.

To explore whether the measures of the observed hub and white matter tracts could successfully predict the ability of semantic processing in the semantic dementia patients, we conducted a series of linear regression analyses, in which node/tract measure was treated as the independent variable, semantic index as the dependent variable, and demographic variables as covariates of non-interest (Supplementary material). The results of these regression analyses were highly convergent with those of correlation analyses (Supplementary material).

Data availability

The data that support the findings of this study are available from the corresponding author, upon reasonable request.

Results

Behavioural performance of participants

The participants' raw accuracies and the corrected t-scores on the behavioural tasks are shown in Table 1. Compared with healthy controls, the semantic dementia group exhibited profound deficits in the general semantic tasks (t-values < -3.5) and in all modality-specific semantic tasks (t-values < -1.5), except the non-verbal motion verification task ($t > -0.5$). By contrast, they performed normally on the three non-semantic control tasks (t-values > -1). These results indicated that the patients presented selective disruptions of general and modality-specific semantic knowledge.

Three components were extracted from the PCA based on six general semantic tasks and three control tasks (Supplementary Table 2). Component 1 accounted for 46% of the model variance, with six general semantic tasks having higher loading weights (0.64 to 0.94) and three control tasks having lower loading weights (–0.09 to 0.00). We thus labelled this component as the semantic processing component and derived scores for each patient's general semantic processing ability based on this component. Component 2 (accounting for 19% of model variance) and Component 3 (15% of model variance) were treated as perceptual and arithmetic components because of their respective heavier loading weight on the visual/sound perception tasks (0.79 to 0.80) and the number proximity matching task (0.94).

Cerebral atrophy of patients

Figure 1 illustrates the comparison of the grey matter volume values between the patients with semantic dementia and healthy control subjects (FDR corrected $q < 0.01$). The patients showed the most severe atrophy in the bilateral ATLs, and the atrophy extended into the more posterior temporal lobes, insula and ventral frontal lobes.

Semantic hub region

Figure 2 shows the white matter anatomical network of the healthy subjects, which contained 90 AAL regions and 457 effective tracts (voxel value $> 25\%$ of subjects, cluster size > 300 voxels). To identify the semantic hub region, we correlated the semantic PCA scores with the nodal degree value for each white matter integrity metric of each region across the 33 patients with semantic dementia, partialling out three
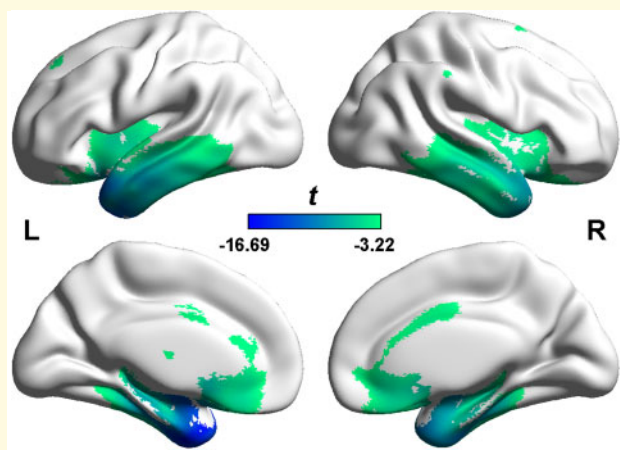
Figure 1 Atrophy map of the semantic dementia patients. The figure shows the areas with significant differences in grey matter volume between the semantic dementia patients and healthy control subjects (FDR-corrected $q < 0.01$).

Figure 2 Whole-brain structural network. A total of 457 tracts were successfully tracked between the 90 regions in 20 healthy subjects, resulting in a whole-brain anatomical network.
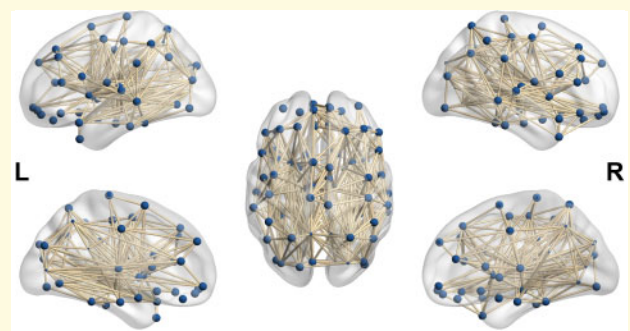
demographic variables (age, gender and educational level). The results are displayed in Fig. 3. No region showed a significant effect under the fractional anisotropy metric. However, for the other three metrics (mean, axial and radial diffusivity), we consistently observed significant negative correlation effects in the left FFG (partial r-values < -0.68, Bonferroni corrected P-values < 0.005; Fig. 3). Furthermore, the correlations in the left FFG remained significant even when we additionally regressed out total grey matter volume (partial r-values < -0.68, P-values < 0.00005), grey matter volume of the left FFG (partial r-values < -0.43, P-values < 0.02) and the t-scores of the three control tasks (partial r-values < -0.70, P-values < 0.00005). These results suggest that the left FFG is a semantic hub region whose disconnection with other regions causes general semantic impairments in semantic dementia.

Semantic-relevant connectivity of the semantic hub

The left FFG in the network connected to nine regions in the temporal, occipital and limbic areas (Fig. 3). These regions were all located in the left hemisphere, including the left superior temporal pole, hippocampus, parahippocampal gyrus, inferior temporal gyrus, middle temporal gyrus, lingual gyrus, calcarine, inferior occipital gyrus, and middle occipital gyrus. Here, we further examined which of the nine white matter tracts contributed to general semantic processing or modality-specific semantic processing.

General semantic-relevant connections of the semantic hub

To explore the general semantic connections of the semantic hub, we tested the correlation between the semantic PCA scores and the diffusion metrics (fractional anisotropy, and

mean, axial and radial diffusivity) of each of the nine connections of the left FFG in 33 patients with semantic dementia. As illustrated in Fig. 4, we did not observe significant effects of any tract for the fractional anisotropy metric. However, we found that the integrity of all nine tracts correlated with semantic PCA scores for the other three metrics (partial r-values < -0.56, Bonferroni corrected P-values < 0.05) (Table 2 and Fig. 4).

We observed nine general semantic connections connected with the left fusiform semantic hub. Here, we investigated whether the significant effects of the observed semantic tracts could be explained by the total grey matter volume or grey matter volume of the node regions and whether the effects were specific to semantic processing. The validation analyses obtained similar results across the three diffusivity metrics. We present only the results of the mean diffusivity metric for simplicity (Table 3). The mean diffusivity of all tracts remained significantly correlated with the semantic PCA scores after partialling out the influence of age, gender, educational level and total grey matter volume (partial r-values < -0.59, P-values < 0.0008) and t-scores of the three non-semantic tasks (partial r-values < -0.60, P-values < 0.001). Most correlations remained after regressing out age, gender, educational level and grey matter volume of the left FFG or the other node (partial r-values < -0.38, P-values < 0.04), except that the effect of three tracts (left FFG-left calcarine, left FFG-left lingual gyrus and left FFG-left superior temporal pole) became weakened when controlling for grey matter volume of the left FFG or the left superior temporal pole ($-0.35 < r$-values < -0.28, $0.07 < P$-values < 0.14).

Modality-specific semantic connections of the semantic hub

To explore the modality-specific semantic connections, we correlated the diffusion measures of each of the nine tracts of the left FFG with the behavioural scores of the 12 tasks covering six semantic modalities, co-varying age, gender, educational level and semantic PCA scores. The analysis revealed that only the axial diffusivity value of the left FFG-
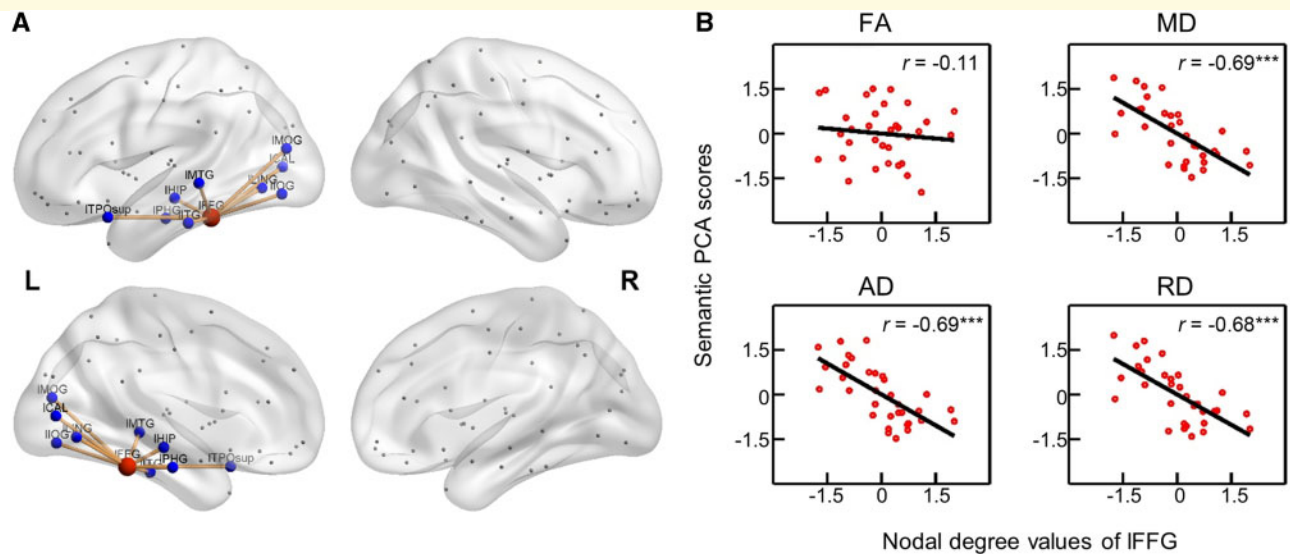
Figure 3 The semantic hub region. (**A**) The left FFG, which was connected with the left superior temporal pole (ITPOsup), hippocampus (IHIP), parahippocampal gyrus (IPHG), inferior temporal gyrus (IITG), middle temporal gyrus (IMTG), lingual gyrus (ILING), calcarine (ICAL), inferior occipital gyrus (IIOG), and middle occipital gyrus (IMOG), was the semantic hub region. (**B**) For three diffusivity metrics [mean, axial and radial diffusivity (MD, AD and RD)], the nodal degree values of the left FFG could significantly predict the semantic PCA scores of the patients (Bonferroni-corrected $P < 0.005$). However, this effect was not observed for the fractional anisotropy (FA) metric. ***Bonferroni-corrected $P < 0.005$.

left calcarine tract correlated significantly ($P < 0.005$) with the scores of the colour matching task (axial diffusivity: partial $r = -0.56$, $P = 0.002$; mean diffusivity: partial $r = -0.50$, $P = 0.006$; radial diffusivity: partial $r = -0.43$, $P = 0.02$; fractional anisotropy: partial $r = -0.14$, $P = 0.46$) (Fig. 5). The effect of this tract held even when introducing more covariates: total grey matter volume (partial $r = -0.57$, $P = 0.002$), grey matter volume of the left FFG (partial $r = -0.56$, $P = 0.002$), grey matter volume of the left calcarine (partial $r = -0.56$, $P = 0.002$), or scores of three non-semantic tasks (partial $r = -0.65$, $P = 0.0004$).

Discussion

Using diffusion-weighted data and semantic behavioural data from 33 patients with semantic dementia, we investigated the semantic hub and semantic connections between the hub and modality-specific regions in the semantic network. We found that the left FFG was the semantic hub as its structural connectivity strength, measured by nodal degree values in the whole brain network, could predict general semantic processing of the patients. This region functions together with nine other regions (the left superior temporal pole, hippocampus, parahippocampal gyrus, inferior temporal gyrus, middle temporal gyrus, lingual gyrus, calcarine, inferior occipital gyrus and middle occipital gyrus) in the semantic memory network. The structural connectivity between the left FFG and these regions correlated significantly with the patients' general semantic performance. Moreover, the connection between the hub and the left

calcarine was involved in colour knowledge processing because the structural connectivity between the left FFG and calcarine could predict colour modality-specific semantic deficits. Our findings provide new supportive evidence for the hub-and-spoke theory of the semantic system from a network perspective.

The semantic hub: the left fusiform gyrus

As a semantic hub, the left FFG plays a core role in binding the information from the distributed modality-specific regions. We found that the disconnection of the hub could cause general semantic deficits in semantic dementia. This replicates the findings of the literature, which also identified the critical role of the left FFG in semantic processing. For example, distortion-corrected functional MRI studies consistently observed activation of this region when healthy subjects performed semantic tasks (Binney et al., 2010; Visser et al., 2010; Visser and Lambon Ralph, 2011; Rice et al., 2015b). Moreover, studies with multivariate pattern analysis also discovered that the left FFG could encode information of semantic categories across verbal and non-verbal modalities (e.g. Fairhall and Caramazza, 2013). Other studies on semantic dementia have also revealed that both metabolism and atrophy of the FFG were associated with semantic processing in semantic dementia (Butler et al., 2009; Mion et al., 2010). However, these neuroimaging and neuropsychological studies only considered the effects of the FFG as a local
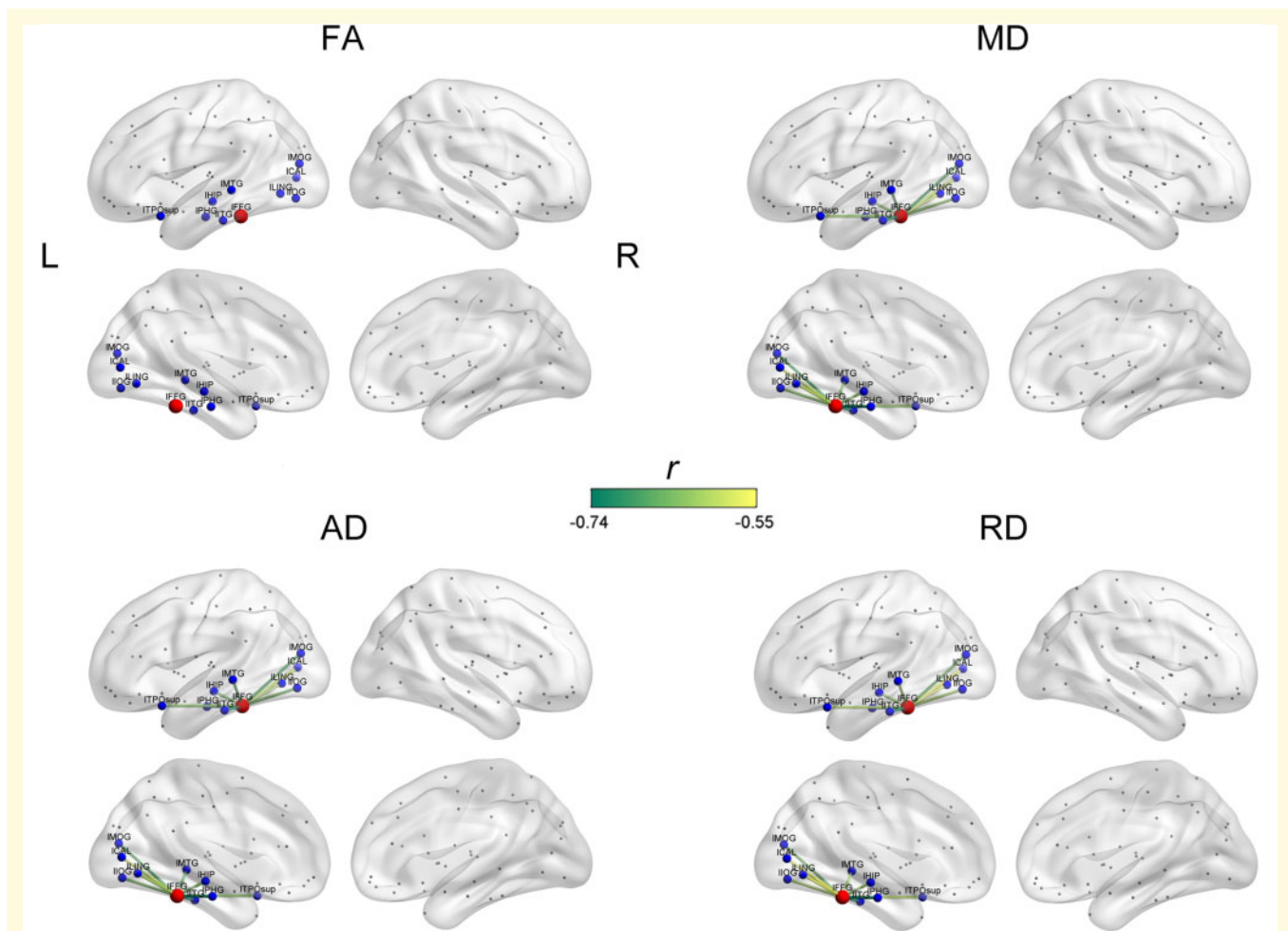
Figure 4 The general semantic-relevant connections of the semantic hub. Three diffusivity metrics [mean, axial and radial diffusivity (MD, AD and RD)] of the nine connections of the left fusiform significantly correlated with the semantic PCA scores in the semantic dementia patients (Bonferroni-corrected $P < 0.05$). However, no effect of any tract was found with the fractional anisotropy (FA) metric. lCAL = calcarine; lHIP = hippocampus; lIOG = inferior occipital gyrus; lITG = inferior temporal gyrus; lLING = lingual gyrus; lMOG = middle occipital gyrus; lMTG = middle temporal gyrus; lPHG = parahippocampal gyrus; lTPOsup = left superior temporal pole; STG = superior temporal gyrus.

Table 2 Correlations between the diffusion metric-values of the tracts and the semantic PCA scores in 33 patients with semantic dementia

White matter connections	Fractional anisotropy		Mean diffusivity		Axial diffusivity		Radial diffusivity	
	r-value	*P*-value	*r*-value	*P*-value	*r*-value	*P*-value	*r*-value	*P*-value
Left FFG-left superior temporal pole	−0.12	0.55	−0.63	0.0003***	−0.64	0.0002***	−0.61	0.0004***
Left FFG-left hippocampus	−0.02	0.91	−0.64	0.0002***	−0.65	0.0002***	−0.63	0.0003***
Left FFG-left parahippocampal gyrus	0.07	0.71	−0.74	0.000004***	−0.74	0.000004***	−0.74	0.000004***
Left FFG-left inferior temporal gyrus	−0.08	0.70	−0.72	0.000007***	−0.71	0.00002***	−0.72	0.000008***
Left FFG-left middle temporal gyrus	−0.17	0.39	−0.65	0.0002***	−0.66	0.00007***	−0.62	0.0003***
Left FFG-left lingual gyrus	−0.09	0.64	−0.60	0.0006***	−0.60	0.0005***	−0.57	0.002***
Left FFG-left calcarine	−0.19	0.31	−0.59	0.0006***	−0.60	0.0005***	−0.56	0.002***
Left FFG-left inferior occipital gyrus	−0.11	0.58	−0.64	0.0002***	−0.66	0.00009***	−0.61	0.0004***
Left FFG-left middle occipital gyrus	−0.15	0.43	−0.68	0.00004***	−0.67	0.00005***	−0.66	0.00009***

***Bonferroni-corrected $P < 0.05$.

region, and did not directly clarify the pivotal role of this region in combining multimodal information within the semantic network. The present study revealed the significant

correlation between the nodal degree of the left FFG and semantic behaviour in patients with semantic dementia, thus providing supportive evidence for the function of the

Table 3 Partial correlation results

White matter connections	Variables							
	Total grey matter volume		Grey matter volume of the left fusiform		Grey matter volume of the other node		Scores of three non-semantic tasks	
	r-value	*P*-value	*r*-value	*P*-value	*r*-value	*P*-value	*r*-value	*P*-value
Left FFG-left superior temporal pole	−0.63	0.0003***	−0.40	0.04*	−0.29	0.13	−0.65	0.0003***
Left FFG-left hippocampus	−0.64	0.0002***	−0.40	0.04*	−0.51	0.005**	−0.66	0.0002***
Left FFG-left parahippocampal gyrus	−0.74	0.000005***	−0.54	0.003**	−0.55	0.003**	−0.77	0.000003***
Left FFG-left inferior temporal gyrus	−0.72	0.00001***	−0.49	0.007**	−0.51	0.005**	−0.75	0.000007***
Left FFG-left middle temporal gyrus	−0.65	0.0002***	−0.40	0.04*	−0.50	0.006**	−0.66	0.0002***
Left FFG-left lingual gyrus	−0.60	0.0006***	−0.28	0.14	−0.56	0.002**	−0.61	0.0008***
Left FFG-left calcarine	−0.59	0.0008***	−0.35	0.07	−0.58	0.001***	−0.60	0.001***
Left FFG-left inferior occipital gyrus	−0.63	0.0003***	−0.38	0.04*	−0.58	0.001***	−0.67	0.0002***
Left FFG-left middle occipital gyrus	−0.68	0.00006***	−0.44	0.02*	−0.65	0.0002***	−0.70	0.00005***

Partial correlation between the mean diffusivity of the tracts and the semantic PCA scores in the semantic dementia patients after additionally controlling for potential confounding factors (total grey matter volume, grey matter volume of the left fusiform, grey matter volume of the other node, and scores of the three non-semantic tasks).
*$P < 0.05$, **$P < 0.01$, ***$P < 0.001$.

Figure 5 The colour modality-specific semantic-relevant connections of the semantic hub. The axial diffusivity (AD) of the connection between the left FFG and left calcarine significantly correlated with the colour matching scores in semantic dementia patients ($P < 0.005$). No effect of any tract was found with the other three metrics or with other modality-specific semantic tasks. FA = fractional anisotropy; lCAL = calcarine; lHIP = hippocampus; lIOG = inferior occipital gyrus; lITG = inferior temporal gyrus; lLING = lingual gyrus; lMOG = middle occipital gyrus; lMTG = middle temporal gyrus; lPHG = parahippocampal gyrus; lTPOsup = left superior temporal pole; MD = mean diffusivity; RD = radial diffusivity; STG = superior temporal gyrus.

left FFG in binding information from various brain regions.

It is worth noting that the anterior portion of the FFG is a homologue of the perirhinal cortex in animals (Insausti *et al.*, 1998; Mion *et al.*, 2010). Studies have uncovered that monkeys with selective perirhinal cortex lesions showed impairments in discriminating complex objects but not simple features such as colour, shape and size (Buckley *et al.*, 2001; Bussey *et al.*, 2002, 2003). This indicates the critical role this region plays in the representations of complex conjunctions of features, which is also analogous to the function of semantic hub in the human brain (Taylor *et al.*, 2006).

In the current study, the semantic hub was observed in unilateral but not bilateral ATLs. This is inconsistent with the hub-and-spoke theory which speculates a bilateral hub representation (Mion *et al.*, 2010; Rice *et al.*, 2015a; Lambon Ralph *et al.*, 2016). The null results of the right ATL in our study might be due to the following reasons. First, it came from insensitive non-verbal semantic measures. Although, bilateral ATLs are involved in semantic processing, the left ATL is more involved in verbal tasks, while the right ATL is more involved in non-verbal tasks (Mion *et al.*, 2010; Gainotti, 2015; Rice *et al.*, 2015b). As our semantic dementia patients were less impaired in non-verbal tasks than in verbal tasks (Bozeat *et al.*, 2000 and see the *t*-scores in Table 1), the neural correlates of the non-verbal component (i.e. the right ATL) became difficult to be detected. Second, the right ATL is mainly responsible for abstract semantic processing (Rice *et al.*, 2015a, b). The stimuli of the current study only included concrete objects, leading to null effects of the right ATL. Finally, the right ATL might be a local semantic region. Given that our study adopted a network perspective to investigate the semantic function of brain regions, the right ATL was not revealed.

Note that semantic disorders could also be observed in patients at the early stages of semantic dementia who exhibited only obvious temporal pole atrophy, and in healthy subjects whose temporal pole regions were temporarily disrupted with repetitive transcranial magnetic stimulation (Pobric *et al.*, 2007; Lambon Ralph *et al.*, 2009; Collins *et al.*, 2017). However, the critical role of the temporal pole in semantic processing was not observed in the current study. This might be due to the following reasons. First, the temporal pole might also be a semantic hub, but may play a different role from the FFG in semantic processing. The temporal pole might be a hub for specific-level semantic knowledge (Grabowski *et al.*, 2001; Damasio *et al.*, 2004; Clarke and Tyler, 2014), while the FFG is a hub for basic-level semantic knowledge (Binney *et al.*, 2010; Mion *et al.*, 2010). The evidence is mainly derived from the fact that the temporal pole is associated with unique entities naming in healthy subjects and in patients (Grabowski *et al.*, 2001; Damasio *et al.*, 2004; Pobric *et al.*, 2007; Tranel, 2009). Because our semantic tasks only tested the effects of semantic knowledge at a general level, the role of the temporal pole was not discovered. Second, the temporal pole might be a semantic hub, and may have a similar role to the FFG.

The hub role of this region was not revealed because of the floor effects of its severe atrophy in our patients. Finally, the temporal pole might not be a semantic hub. When the temporal pole shows visible atrophy, the FFG might also have been damaged in semantic dementia. The damage of the FFG might cause the patients' semantic impairments. Similarly, repetitive transcranial magnetic stimulation over the temporal pole might also inhibit the function of the FFG because the two brain regions are anatomically close.

Semantic connectivity of the hub region

White matter tractography results revealed that the left FFG was linked with the temporal area (superior temporal pole, inferior temporal gyrus, and middle temporal gyrus), limbic area (hippocampus, parahippocampal gyrus), and occipital area (lingual gyrus, calcarine, inferior occipital gyrus, middle occipital gyrus) with white matter connections. This is consistent with previous studies (Acosta-Cabronero *et al.*, 2011; Zhou *et al.*, 2012; Guo *et al.*, 2013) that also identified white matter connectivity between these areas.

Prior studies have shown that these connections are damaged in semantic dementia (Acosta-Cabronero *et al.*, 2011). However, it could not be concluded whether those connections had a semantic function or the damage was just a by-product of the disease. This study further revealed that all the connections were associated with semantic impairments in the patients with semantic dementia. We postulate that the distributed regions play different roles in the semantic system. The temporal pole might store concepts of unique entities such as famous people or buildings (Pobric *et al.*, 2007; Clarke and Tyler, 2014; Montembeault *et al.*, 2017). The medial temporal lobe limbic system, including the hippocampus and parahippocampal gyrus, acts as a memory-based stimulation system and re-enacts the modality-specific regions during concept retrieval (Bates *et al.*, 2003; Schacter *et al.*, 2007; Xu *et al.*, 2016). Other temporal and occipital regions represent modality-specific knowledge, such as object form and colour.

Of all these connections, the left FFG-left calcarine was observed to devote to the processing of colour-specific knowledge in this study. The left calcarine has been confirmed to subserve colour processing. One of the most compelling pieces of evidence comes from a case study by Miceli *et al.* (2001). They found that Patient I.O.C., who had lesions in the left calcarine, had intact colour recognition but impaired retrieval of colour knowledge. Our study further revealed that the fibre bundle between the calcarine and the semantic hub was important for colour knowledge processing. This study also elucidated the white matter basis for the colour-specific deficits of semantic dementia, which has been behaviourally observed in the literature (Hoffman *et al.*, 2012).

Limitations

This study has at least the following limitations. First, the cerebral atrophy of our patient sample only covered certain brain areas, and the remaining areas were not examined. Second, the intensity artefacts of the ATL and adjacent orbitofrontal cortex were not well controlled. Future research might use multi-shot methods, parallel imaging, or field-map-based techniques to improve imaging sensitivity of these regions (Jezzard and Balaban, 1995; Griswold *et al.*, 2002; Holdsworth *et al.*, 2008). Third, the number of diffusion weighting directions was relatively low, and as a result, the accuracy of the obtained tracts might not be optimal. More gradient directions (>60), in addition to more complex acquisition profiles (e.g. HARDI; Tuch *et al.*, 2002), are required in future studies. Finally, the effects of the left FFG could only be observed under three diffusivity metrics and not under fractional anisotropy. This might be because the fractional anisotropy metric is not a sensitive measurement in revealing white matter damage in neurodegenerative disorders such as semantic dementia (e.g. Acosta-Cabronero *et al.*, 2010, 2011). This needs to be elucidated in future research.

Conclusions

By investigating the relationship between general and modality-specific semantic performance and nodal degree of the regions and diffusion metrics of the connections in semantic dementia, we identified the semantic hub and semantic connections within the hub-and-spoke semantic network. The left FFG is the hub of the network. This region works together with nine regions for general semantic processing and functions with the left calcarine for colour modality-specific semantic processing. These results provide new evidence for the organization of semantic memory on the basis of the semantic dementia lesion model, thereby deepening our understanding of the neuroanatomical network of semantic processing.

Acknowledgements

We would like to thank our anonymous reviewers for thoughtful comments on the manuscript, Yanchao Bi for elaborate design of behavioural tasks, Gaolang Gong, Yuxing Fang and Mingyang Li for optimization of imaging methodology, Yuhan Lu and Anqi Dai for help with English editing. We are also grateful to all research participants.

Funding

Competing interests

The authors report no competing interests.

Supplementary material

Supplementary material is available at *Brain* online.

References

Achard S, Bullmore E. Efficiency and cost of economical brain functional networks. PLoS Comput Biol 2007; 3: e17.

Achard S, Salvador R, Whitcher B, Suckling J, Bullmore E. A resilient, low-frequency, small-world human brain functional network with highly connected association cortical hubs. J Neurosci 2006; 26: 63–72.

Acosta-Cabronero J, Patterson K, Fryer TD, Hodges JR, Pengas G, Williams GB, et al. Atrophy, hypometabolism and white matter abnormalities in semantic dementia tell a coherent story. Brain 2011; 134: 2025–35.

Acosta-Cabronero J, Williams GB, Pengas G, Nestor PJ. Absolute diffusivities define the landscape of white matter degeneration in Alzheimer's disease. Brain 2010; 133: 529–39.

Agosta F, Henry RG, Migliaccio R, Neuhaus J, Miller BL, Dronkers NF, et al. Language networks in semantic dementia. Brain 2010; 133: 286–99.

Andreotti J, Dierks T, Wahlund LO, Grieder M. Diverging progression of network disruption and atrophy in Alzheimer's disease and semantic dementia. J Alzheimer's Dis 2017; 55: 981–93.

Ashburner J. A fast diffeomorphic image registration algorithm. Neuroimage 2007; 38: 95–113.

Bates E, Wilson SM, Saygin AP, Dick F, Sereno MI, Knight RT, et al. Voxel-based lesion–symptom mapping. Nat Neurosci 2003; 6: 448–50.

Binder JR, Desai RH, Graves WW, Conant LL. Where is the semantic system? A critical review and meta-analysis of 120 functional neuroimaging studies. Cereb Cortex 2009; 19: 2767–96.

Binney RJ, Embleton KV, Jefferies E, Parker GJM, Lambon Ralph MA. The ventral and inferolateral aspects of the anterior temporal lobe are crucial in semantic memory: evidence from a novel direct comparison of distortion-corrected fMRI, rTMS, and semantic dementia. Cereb Cortex 2010; 20: 2728–38.

Bozeat S, Lambon Ralph MA, Patterson K, Garrard P, Hodges JR. Non-verbal semantic impairment in semantic dementia. Neuropsychologia 2000; 38: 1207–15.

Buckley MJ, Booth MC, Rolls ET, Gaffan D. Selective perceptual impairments after perirhinal cortex ablation. J Neurosci 2001; 21: 9824–36.

Bussey TJ, Saksida LM, Murray EA. Perirhinal cortex resolves feature ambiguity in complex visual discriminations. Eur J Neurosci 2002; 15: 365–74.

Bussey TJ, Saksida LM, Murray EA. Impairments in visual discrimination after perirhinal cortex lesions: testing 'declarative' vs. 'perceptual-mnemonic' views of perirhinal cortex function. Eur J Neurosci 2003; 17: 649–60.

Butler CR, Brambati SM, Miller BL, Gorno-Tempini ML. The neural correlates of verbal and non-verbal semantic processing deficits in neurodegenerative disease. Cogn Behav Neurol 2009; 22: 73–80.

Chen Y, Chen K, Ding J, Zhang Y, Yang Q, Lv Y, et al. Neural substrates of amodal and modality-specific semantic processing within

the temporal lobe: a lesion-behavior mapping study of semantic dementia. Cortex 2019; 120: 78–91.

Cheng H, Wang Y, Sheng J, Sporns O, Kronenberger WG, Mathews VP, et al. Optimization of seed density in DTI tractography for structural networks. J Neurosci Methods 2012; 203: 264–72.

Clarke A, Tyler LK. Object-specific semantic coding in human perirhinal cortex. J Neurosci 2014; 34: 4766–75.

Collins JA, Montal V, Hochberg D, Quimby M, Mandelli ML, Makris N, et al. Focal temporal pole atrophy and network degeneration in semantic variant primary progressive aphasia. Brain 2017; 140: 457–71.

Crawford JR, Garthwaite PH. Comparing patients' predicted test scores from a regression equation with their obtained scores: a significance test and point estimate of abnormality with accompanying confidence limits. Neuropsychology 2006; 20: 259.

Cui Z, Zhong S, Xu P, He Y, Gong G. PANDA: a pipeline toolbox for analyzing brain diffusion images. Front Hum Neurosci 2013; 7: 42.

Damasio H, Tranel D, Grabowski T, Adolphs R, Damasio A. Neural systems behind word and concept retrieval. Cognition 2004; 92: 179–229.

Ding J, Chen K, Chen Y, Fang Y, Yang Q, Lv Y, et al. The left fusiform gyrus is a critical region contributing to the core behavioral profile of semantic dementia. Front Hum Neurosci 2016; 10: 215.

Fairhall SL, Caramazza A. Brain regions that represent amodal conceptual knowledge. J Neurosci 2013; 33: 10552–8.

Fang Y, Han Z, Zhong S, Gong G, Song L, Liu F, et al. The semantic anatomical network: evidence from healthy and brain-damaged patient populations. Hum Brain Mapp 2015; 36: 3499–515.

Folstein MF, Folstein SE, McHugh PR. "Mini-mental state": a practical method for grading the cognitive state of patients for the clinician. J Psychiatr Res 1975; 12: 189–98.

Freeman LC. A set of measures of centrality based on betweenness. Sociometry 1977; 40: 35–41.

Gainotti G. Is the difference between right and left ATLs due to the distinction between general and social cognition or between verbal and nonverbal representations? Neurosci Biobehav Rev 2015; 51: 296–312.

Golden HL, Downey LE, Fletcher PD, Mahoney CJ, Schott JM, Mummery CJ, et al. Identification of environmental sounds and melodies in syndromes of anterior temporal lobe degeneration. J Neurol Sci 2015; 352: 94–8.

Gong G, He Y, Concha L, Lebel C, Gross DW, Evans AC, et al. Mapping anatomical connectivity patterns of human cerebral cortex using in vivo diffusion tensor imaging tractography. Cereb Cortex 2009; 19: 524–36.

Gorno-Tempini ML, Hillis AE, Weintraub S, Kertesz A, Mendez M, Cappa SF, et al. Classification of primary progressive aphasia and its variants. Neurology 2011; 76: 1006–14.

Grabowski TJ, Damasio H, Tranel D, Boles Ponto LL, Hichwa RD, Damasio AR. A role for left temporal pole in the retrieval of words for unique entities. Hum Brain Mapp 2001; 13: 199–212.

Griswold MA, Jakob PM, Heidemann RM, Nittka M, Jellus V, Wang J, et al. Generalized autocalibrating partially parallel acquisitions (GRAPPA). Magn Reson Med 2002; 47: 1202–10.

Guo CC, Gorno-Tempini ML, Gesierich B, Henry M, Trujillo A, Shany-Ur T, et al. Anterior temporal lobe degeneration produces widespread network-driven dysfunction. Brain 2013; 136: 2979–91.

Han Z, Ma Y, Gong G, He Y, Caramazza A, Bi Y. White matter structural connectivity underlying semantic processing: evidence from brain damaged patients. Brain 2013; 136: 2952–65.

He Y, Chen Z, Gong G, Evans A. Neuronal networks in Alzheimer's disease. Neuroscientist 2009; 15: 333–50.

Hoffman P, Jones RW, Lambon Ralph MA. The degraded concept representation system in semantic dementia: damage to pan-modal hub, then visual spoke. Brain 2012; 135: 3770–80.

Holdsworth SJ, Skare S, Newbould RD, Guzmann R, Blevins NH, Bammer R. Readout-segmented EPI for rapid high resolution diffusion imaging at 3T. Eur J Radiol 2008; 65: 36–46.

Insausti R, Juottonen K, Soininen H, Insausti AM, Partanen K, Vainio P, et al. MR volumetric analysis of the human entorhinal, perirhinal, and temporopolar cortices. AJNR Am J Neuroradiol 1998; 19: 659–71.

Jefferies E, Patterson K, Jones RW, Lambon Ralph MA. Comprehension of concrete and abstract words in semantic dementia. Neuropsychology 2009; 23: 492–9.

Jezzard P, Balaban RS. Correction for geometric distortion in echo planar images from B0 field variations. Magn Reson Med 1995; 34: 65–73.

Lambon Ralph MA. Neurocognitive insights on conceptual knowledge and its breakdown. Philos Trans R Soc B-Biol Sci 2014; 369: 2012392.

Lambon Ralph MA, Jefferies E, Patterson K, Rogers TT. The neural and computational bases of semantic cognition. Nat Rev Neurosci 2016; 18: 42–55.

Lambon Ralph MA, Pobric G, Jefferies E. Conceptual knowledge is underpinned by the temporal pole bilaterally: convergent evidence from rTMS. Cereb Cortex 2009; 19: 832–8.

Lambon Ralph MA, Sage K, Jones RW, Mayberry EJ. Coherent concepts are computed in the anterior temporal lobes. Proc Natl Acad Sci U S A 2010; 107: 2717–22.

Lin N, Guo Q, Han Z, Bi Y. Motor knowledge is one dimension for concept organization: further evidence from a Chinese semantic dementia case. Brain Lang 2011; 119: 110–8.

Luzzi S, Snowden JS, Neary D, Coccia M, Provinciali L, Lambon Ralph MA. Distinct patterns of olfactory impairment in Alzheimer's disease, semantic dementia, frontotemporal dementia, and corticobasal degeneration. Neuropsychologia 2007; 45: 1823–31.

Martin A. The representation of object concepts in the brain. Annu Rev Psychol 2007; 58: 25–45.

Martin A. GRAPES—Grounding representations in action, perception, and emotion systems: how object properties and categories are represented in the human brain. Psychon Bull Rev 2016; 23: 979–90.

Mesulam M-M, Wieneke C, Thompson C, Rogalski E, Weintraub S. Quantitative classification of primary progressive aphasia at early and mild impairment stages. Brain 2012; 135: 1537–53.

Miceli G, Fouch E, Capasso R, Shelton JR, Tomaiuolo F, Caramazza A. The dissociation of color from form and function knowledge. Nat Neurosci 2001; 4: 662–7.

Mion M, Patterson K, Acosta-Cabronero J, Pengas G, Izquierdo-Garcia D, Hong YT, et al. What the left and right anterior fusiform gyri tell us about semantic memory. Brain 2010; 133: 3256–68.

Montembeault M, Brambati SM, Joubert S, Boukadi M, Chapleau M, Laforce R, et al. Naming unique entities in the semantic variant of primary progressive aphasia and Alzheimer's disease: towards a better understanding of the semantic impairment. Neuropsychologia 2017; 95: 11–20.

Mori S, Crain BJ, Chacko VP, Van Zijl PC. Three-dimensional tracking of axonal projections in the brain by magnetic resonance imaging. Ann Neurol 1999; 45: 265–9.

Patterson K, Nestor PJ, Rogers TT. Where do you know what you know? The representation of semantic knowledge in the human brain. Nat Rev Neurosci 2007; 8: 976–87.

Pobric G, Jefferies E, Lambon Ralph MA. Anterior temporal lobes mediate semantic representation: mimicking semantic dementia by using rTMS in normal participants. Proc Natl Acad Sci U S A 2007; 104: 20137–41.

Rice GE, Caswell H, Moore P, Hoffman P, Lambon Ralph MA. The roles of left versus right anterior temporal lobes in semantic memory: a neuropsychological comparison of postsurgical temporal lobe epilepsy patients. Cereb Cortex 2018; 28: 1487–501.

Rice GE, Hoffman P, Lambon Ralph MA. Graded specialization within and between the anterior temporal lobes. Ann NY Acad Sci 2015; 1359: 84–97.

Rice GE, Lambon Ralph MA, Hoffman P. The roles of left versus anterior temporal lobes in conceptual knowledge: an ALE meta-analysis of 97 functional neuroimaging studies. Cereb Cortex 2015; 25: 4374–91.

Rogers TT, Lambon Ralph MA, Garrard P, Bozeat S, McClelland JL, Hodges JR, et al. Structure and deterioration of semantic memory: a neuropsychological and computational investigation. Psychol Rev 2004; 111: 205–35.

Schacter DL, Addis DR, Buckner RL. Remembering the past to imagine the future: the prospective brain. Nat Rev Neurosci 2007; 8: 657–61.

Schapiro AC, McClelland JL, Welbourne SR, Rogers TT, Lambon Ralph MA. Why bilateral damage is worse than unilateral damage to the brain. J Cogn Neurosci 2013; 25: 2107–23.

Snowden JS, Thompson JC, Neary D. Knowledge of famous faces and names in semantic dementia. Brain 2004; 127: 860–72.

Taylor KI, Moss HE, Stamatakis EA, Tyler LK. Binding crossmodal object features in perirhinal cortex. Proc Natl Acad Sci U S A 2006; 103: 8239–44.

Tranel D. The left temporal pole is important for retrieving words for unique concrete entities. Aphasiology 2009; 23: 867–84.

Tuch DS, Reese TG, Wiegell MR, Makris N, Belliveau JW, Wedeen VJ. High angular resolution diffusion imaging reveals intravoxel white matter fiber heterogeneity. Magn Reson Med 2002; 48: 577–82.

Tulving E, Episodic and semantic memory. In: E Tulving, W Donaldson, editors. Organization of memory. London: Academic; 1972. p. 381–403.

Tzourio-Mazoyer N, Landeau B, Papathanassiou D, Crivello F, Etard O, Delcroix N, et al. Automated anatomical labeling of activations in SPM using a macroscopic anatomical parcellation of the MNI MRI single-subject brain. Neuroimage 2002; 15: 273–89.

Visser M, Embleton KV, Jefferies E, Parker GJ, Lambon Ralph MA. The inferior, anterior temporal lobes and semantic memory clarified: novel evidence from distortion-corrected fMRI. Neuropsychologia 2010; 48: 1689–96.

Visser M, Lambon Ralph MA. Differential contributions of bilateral ventral anterior temporal lobe and left anterior superior temporal gyrus to semantic processes. J Cogn Neurosci 2011; 23: 3121–31.

Warrington EK, Shallice T. Category-specific semantic impairments. Brain 1984; 107: 829–54.

Xu Y, Lin Q, Han Z, He Y, Bi Y. Intrinsic functional network architecture of human semantic processing: modules and hubs. Neuroimage 2016; 132: 542–55.

Zhou J, Gennatas ED, Kramer JH, Miller BL, Seeley WW. Predicting regional neurodegeneration from the healthy brain functional connectome. Neuron 2012; 73: 1216–27.